Spectral Domain Analysis of an Open Slot Ring Resonator

KENJI KAWANO AND HISASHI TOMIMURO

Abstract—**A full wave analysis of an open slot ring resonator on a dielectric substrate is presented. It is based upon Galerkin's method in the Hankel transform domain. The computed resonant frequencies for several slot widths agree well with the experimental values on alumina substrate with $\epsilon_r = 9.6$ in the 26–37-GHz frequency range.**

I. Introduction

MICROSTRIP DISK and ring resonators are utilized as resonators, filters, antennas, and other circuit elements for microwave integrated circuits [1]. These resonators early have been analyzed by a magnetic wall model [2]–[4]. Although this analysis method is simple and useful, more rigorous analyses have been required for more accurate design. Hence many improved analyses have been reported [5]–[7]. Furthermore, Araki and Itoh have developed a rigorous full wave analysis to obtain accurate resonant frequencies and radiation patterns [8]. The analysis is based upon Galerkin's method in the Hankel transform domain.

Meanwhile, the authors have developed slot ring resonators to measure accurate guide wave lengths of slot lines [9]. Although slot ring resonators are considered to be useful as circuit elements for microwave integrated circuits, they have not been analyzed yet.

This paper presents resonant frequencies of an open slot ring resonator determined by the Hankel transform domain analysis. In Section II, dyadic Green functions and the characteristic equation are derived and the sensitivity of the solution with respect to the basis functions is investigated. In Section III, the experimental procedure for alumina substrate is described. In Section IV, the computed resonant frequencies are compared with the measured values. It is shown that the numerical results agree well with the experimental results, especially for wide width region of slots.

II. Analysis Method

A. Green Functions

Fig. 1 shows the slot ring resonator to be analyzed. A ring-like slot line is placed on the bottom surface of the substrate of thickness d. It is assumed that metals are infinitely thin and perfect conductors and that the substrate material, whose permittivity and permeability are ϵ_r and μ_r, respectively, is lossless.

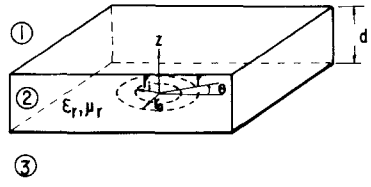

Fig. 1. Slot ring resonator and the coordinate system. ①Upper air region. ②Substrate region. ③Lower air region.

1) Field Expression: The first step is to derive the tangential field components. It is well known that the electromagnetic fields can be obtained from a superposition of TE and TM fields.

The axial field components $E_z(r, \theta, z)$ and $H_z(r, \theta, z)$, which satisfy the Helmholtz equation, can be expressed with the definition of the Hankel transform as follows [10].

A) In upper air region $(z > d)$:

$$E_{z1}(r, \theta, z) = e^{jn\theta} \int_0^\infty A^e(\alpha) e^{-j\beta_1(z-d)} J_n(\alpha r) \alpha d\alpha \quad (1a)$$

$$H_{z1}(r, \theta, z) = e^{jn\theta} \int_0^\infty A^h(\alpha) e^{-j\beta_1(z-d)} J_n(\alpha r) \alpha d\alpha. \quad (1b)$$

B) In substrate region $(d > z > 0)$:

$$E_{z2}(r, \theta, z) = e^{jn\theta} \int_0^\infty \{B^e(\alpha) \sin(\beta_2 z) + C^e(\alpha) \cos(\beta_2 z)\} J_n(\alpha r) \alpha d\alpha \quad (1c)$$

$$H_{z2}(r, \theta, z) = e^{jn\theta} \int_0^\infty \{B^h(\alpha) \sin(\beta_2 z) + C^h(\alpha) \cos(\beta_2 z)\} J_n(\alpha r) \alpha d\alpha. \quad (1d)$$

C) In lower air region $(0 > z)$:

$$E_{z3}(r, \theta, z) = e^{jn\theta} \int_0^\infty D^e(\alpha) e^{j\beta_3 z} J_n(\alpha r) \alpha d\alpha \quad (1e)$$

$$H_{z3}(r, \theta, z) = e^{jn\theta} \int_0^\infty D^h(\alpha) e^{j\beta_3 z} J_n(\alpha r) \alpha d\alpha \quad (1f)$$

where subscripts 1, 2, and 3 designate the upper air, substrate and lower air region, and

$$\beta_1^2 = \omega^2 \epsilon_1 \mu_1 - \alpha^2 \quad \beta_2^2 = \omega^2 \epsilon_2 \mu_2 - \alpha^2$$

$$\beta_3^2 = \omega^2 \epsilon_3 \mu_3 - \alpha^2$$

$$\epsilon_1 = \epsilon_3 = \epsilon_0 \quad \epsilon_2 = \epsilon_r \epsilon_0$$

$$\mu_1 = \mu_3 = \mu_0 \quad \mu_2 = \mu_r \mu_0$$

Manuscript received October 2, 1981; revised March 3, 1982.

The authors are with the Component Engineering Section, Musashino Electrical Communication Laboratories, Nippon Telegraph and Telephone Public Corporation, Musashino-shi, Tokyo, 180, Japan.

0018-9480/82/0800-1184$00.75 ©1982 IEEE

where α is the Hankel transform variable, ω is the angular resonant frequency, ϵ_0 and μ_0 are the free space permittivity and permeability. $J_n(\alpha r)$ is the Bessel function of the first kind and nth order. $A^e(\alpha),\cdots,D^h(\alpha)$ are unknown coefficients which are determined from the boundary conditions at the interfaces $z=0$ and $z=d$. The radical and azimuthal field components derived from (1) contain the Bessel functions of $n-1$th order and $n+1$th order because of the derivative with respect to the argument r. Therefore, the following expressions will be used to reduce them to the same order of the Bessel functions:

$$E_{i\pm}(r,\theta,z)=E_{ri}(r,\theta,z)\pm jE_{\theta i}(r,\theta,z) \tag{2a}$$

$$H_{i\pm}(r,\theta,z)=H_{ri}(r,\theta,z)\pm jH_{\theta i}(r,\theta,z) \tag{2b}$$

where $E_{ri}(r,\theta,z)$ and $E_{\theta i}(r,\theta,z)$ are the radical and azimuthal electric field components, respectively, and $H_{ri}(r,\theta,z)$ and $H_{\theta i}(r,\theta,z)$ are the radical and azimuthal magnetic field components, respectively.

2) Boundary Conditions: The second step is to apply the boundary conditions at the interfaces $z=0$ and $z=d$ to obtain Green functions. They are as follows.

a) Top substrate surface ($z=d$): The tangential field components are continuous

$$E_{1\pm}(r,\theta,d)=E_{2\pm}(r,\theta,z) \tag{3a}$$

$$H_{1\pm}(r,\theta,z)=H_{2\pm}(r,\theta,z). \tag{3b}$$

b) Bottom substrate surface ($z=0$): The electric field components are continuous and the magnetic field components are related to the conductor current densities, that is,

$$E_{2\pm}(r,\theta,0)=E_{3\pm}(r,\theta,0)=E_{\pm}(r,\theta,0) \tag{4a}$$

$$J_{\pm}(r,\theta,0)=\pm j\{H_{2\pm}(r,\theta,0)-H_{3\pm}(r,\theta,0)\} \tag{4b}$$

where $E_{\pm}(r,\theta,0)$ and $J_{\pm}(r,\theta,0)$ are the unknown tangential electric field components and conductor current densities, respectively.

From (2), (3), and (4a), $B^e(\alpha)$, $C^e(\alpha)$, $D^e(\alpha)$, $B^h(\alpha)$, $C^h(\alpha)$, and $D^h(\alpha)$ are expressed in terms of the tangential electric field components $E_{\pm}(r,\theta,z)$ at the interface $z=0$.

From these expressions and (4b), the following matrix equation is obtained:

$$\begin{pmatrix}\tilde{G}_{++}(\omega,\alpha) & \tilde{G}_{+-}(\omega,\alpha)\\ \tilde{G}_{-+}(\omega,\alpha) & \tilde{G}_{--}(\omega,\alpha)\end{pmatrix}\cdot\begin{pmatrix}\tilde{E}_{+}(\alpha)\\ \tilde{E}_{-}(\alpha)\end{pmatrix}=\begin{pmatrix}\tilde{J}_{+}(\alpha)\\ \tilde{J}_{-}(\alpha)\end{pmatrix} \tag{5}$$

where $\tilde{J}_{\pm}(\alpha)$ are the Hankel transforms of the conductor current densities $J_{\pm}(r,\theta,z)$ at the interface $z=0$.

Expressions for $\tilde{G}_{++}(\omega,\alpha),\cdots,\tilde{G}_{--}(\omega,\alpha)$ are as follows:

$$\tilde{G}_{++}(\omega,\alpha)=\frac{j\omega\epsilon_2}{2\beta_2}\frac{j\beta_2-\beta_1\epsilon_r\tan(\beta_2 d)}{\beta_1\epsilon_r+j\beta_2\tan(\beta_2 d)}-\frac{\omega\epsilon_3}{2\beta_3}-\frac{j\beta_2}{2\omega\mu_2}\frac{\beta_1\mu_r+j\beta_2\tan(\beta_2 d)}{j\beta_2-\beta_1\mu_r\tan(\beta_2 d)}-\frac{\beta_3}{2\omega\mu_3} \tag{6a}$$

and

$$\tilde{G}_{+-}(\omega,\beta)=-\frac{j\omega\epsilon_2}{2\beta_2}\frac{j\beta_2-\beta_1\epsilon_r\tan(\beta_2 d)}{\beta_1\epsilon_r+j\beta_2\tan(\beta_2 d)}+\frac{\omega\epsilon_3}{2\beta_3}-\frac{j\beta_2}{2\omega\mu_2}\frac{\beta_1\mu_r+j\beta_2\tan(\beta_2 d)}{j\beta_2-\beta_1\mu_r\tan(\beta_2 d)}-\frac{\beta_3}{2\omega\mu_3} \tag{6b}$$

$$\tilde{G}_{-+}(\omega,\alpha)=\tilde{G}_{+-}(\omega,\alpha) \tag{6c}$$

$$\tilde{G}_{--}(\omega,\alpha)=\tilde{G}_{++}(\omega,\alpha) \tag{6d}$$

where $\tilde{G}_{++}(\alpha,\omega),\cdots,\tilde{G}_{--}(\alpha,\omega)$ are the admittance Green functions in the Hankel transform domain.

B. Characteristic Equation

The third step is to derive the characteristic equation. Although the matrix equation (5) contains four unknown functions $\tilde{E}_{\pm}(\alpha)$ and $\tilde{J}_{\pm}(\alpha)$, the functions $\tilde{J}_{\pm}(\alpha)$ can be eliminated by using Galerkin's method in the Hankel transform domain.

First, we expand unknown $\tilde{E}_{\pm}(\alpha)$ in terms of known basis functions $\tilde{E}_{\pm m}(\alpha)$

$$\tilde{E}_{+}(\alpha)=\sum_{m=1}^{M}c_m\tilde{E}_{+m}(\alpha) \tag{7a}$$

$$\tilde{E}_{-}(\alpha)=\sum_{m=1}^{M}d_m\tilde{E}_{-m}(\alpha) \tag{7b}$$

where c_m, d_m are unknown constants.

Next, we substitute (7) into (5) and take inner products with $\tilde{E}_{\pm i}(\alpha)$. Then the following algebraic equations are obtained:

$$\sum_{m=1}^{M}K_{im}^{++}(\omega)c_m+\sum_{m=1}^{M}K_{im}^{+-}(\omega)d_m=0 \qquad (i=1,2,\cdots,) \tag{8a}$$

$$\sum_{m=1}^{M}K_{im}^{-+}(\omega)c_m+\sum_{m=1}^{M}K_{im}^{--}(\omega)d_m=0 \qquad (i=1,2,\cdots,) \tag{8b}$$

where

$$K_{im}^{++}(\omega)=\int_0^{\infty}\tilde{E}_{+i}(\alpha)\tilde{G}_{++}(\omega,\alpha)\tilde{E}_{+m}(\alpha)\alpha d\alpha \tag{9a}$$

$$K_{im}^{+-}(\omega)=\int_0^{\infty}\tilde{E}_{+i}(\alpha)\tilde{G}_{+-}(\omega,\alpha)\tilde{E}_{-m}(\alpha)\alpha d\alpha \tag{9b}$$

$$K_{im}^{-+}(\omega)=\int_0^{\infty}\tilde{E}_{-1}(\alpha)\tilde{G}_{-+}(\omega,\alpha)\tilde{E}_{+m}(\alpha)\alpha d\alpha \tag{9c}$$

$$K_{im}^{--}(\omega)=\int_0^{\infty}\tilde{E}_{-i}(\alpha)\tilde{G}_{--}(\omega,\alpha)\tilde{E}_{-m}(\alpha)\alpha d\alpha. \tag{9d}$$

In the derivation of (8), Parseval's theorem in the Hankel transform domain is used

$$\int_0^{\infty}\tilde{E}_{\pm i}(\alpha)\tilde{J}_{\pm}(\alpha)\alpha d\alpha=\int_0^{\infty}E_{\pm i}(r,\theta,0)J_{\pm}(r,\theta,0)\,rdr=0\,(i=1,2,\cdots,) \tag{10}$$

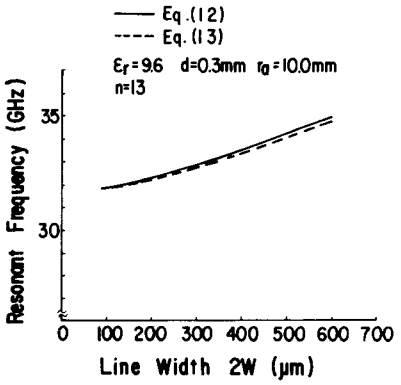

Fig. 2. Resonant frequency of the slot ring resonators for different basis functions as a function of line width. n is the azimuthal resonant order.

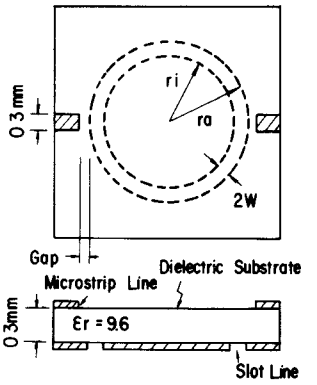

Fig. 3. Experimental geometry for the measurement of a slot ring resonator.

which is valid since the electric field components $E_{\pm}(r,\theta,0)$ and the current densities $J_{\pm}(r,\theta,0)$ are zero in the complementary regions of the interface at $z=0$.

The following characteristic equation for the complex resonant frequency ω_0 is obtained by setting zero the determinant of the coefficient matrix $K(\omega)$. The resonant frequency is obtained from the real part of this quantity

$$\det|K(\omega_0)|=0. \tag{11}$$

C. Basis Functions

As one term approximation using well-behaved basis functions gives good results for infinite slot lines [9],[11], the following basis functions are assumed, that is, the number of the basis functions is only one:

$$E_r(r)=\begin{cases}\dfrac{1}{2W}\left(1+\left|\dfrac{r-r_m}{W}\right|^3\right) & (\text{for}\,|r-r_m|<W)\\ 0 & (\text{for other } r)\end{cases} \tag{12a}$$

$$E_\theta(r)=0 \qquad (\text{for all } r). \tag{12b}$$

In the case of a slot line, the characteristic equation reduces to the evaluation of a single integral when the line-length-directed field component is assumed zero. In the case of a slot ring resonator, however, the characteristic equation contains four integrals even if $E_\theta(r)=0$.

Hence, in order to investigate the sensitivity of the solution with respect to the basis functions, the following functions are assumed in addition to (12):

$$E_r(r)=\begin{cases}1 & (\text{for}\,|r-r_m|<W)\\ 0 & (\text{for other } r)\end{cases} \tag{13a}$$

$$E_\theta(r)=0 \qquad (\text{for all } r) \tag{13b}$$

where $r_m=1/2(r_a+r_i)$.

The Hankel transforms of these functions were obtained by numerical integration. The upper and lower integration limits were determined by the limits of the Bessel function's argument in ECL's computer library.

Fig. 2 shows the numerical results of the 13th-order resonant frequencies versus the slot width. As the difference between both results is small, it is considered that the sensitivity of the solution with respect to the basis functions is relatively small. In computation, the solution

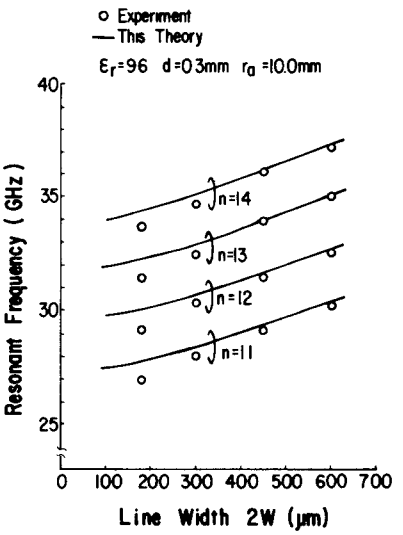

Fig. 4. Theoretical and experimental resonant frequencies for the slot ring resonators as a function of line width. n is the azimuthal resonant order.

for (11) has been obtained by the method of successive bisection. The integration has been performed in the real axis of the complex α plane, avoiding the poles of $\tilde{G}_{++}(\omega,\alpha)$, etc., the matrix elements $K_{1m}^{++}(\omega,\alpha)$, etc. A typical computer time is about 20 s on DIPS-M2.

III. Experimental Procedure

Fig. 3 shows the experimental geometry of a slot ring resonator. Microstrip lines are used for input and output terminals of electromagnetic power on the opposite side of the ring-like slot line. The former is shown as the solid lines and the latter is shown as the dotted lines. The coupling gap between the microstrip lines and the slot line is about 25 μm. The substrate is 25×25×0.3-mm alumina with the relative dielectric constant 9.6. The metals are 0.02 μm thick nickel-chromium and 4-μm thick gold. The widths of the ring-like slot lines studied are 180, 300, 450, and 600 μm. All of them have the same 10-mm outer radius.

IV. Numerical and Experimental Results

Fig. 4 shows the resonant frequencies computed from (12) and the measured resonant frequencies. The frequency range investigated is 26–37 GHz which corresponds to about the 10th resonant order. When slot line width in-

creases, the resonant frequency also increases. This means that one wavelength decreases for wider width slot since the outer radius r_a is constant. The numerical results agree with the experimental results within about 3 percent, especially about 1 percent in the wide linewidth region. It is considered that the sources of the relatively large differences in the narrow line width region are attributed to the basis function. In order to improve the numerical results for this region, more detailed investigation for the basis function is required. Q values for these resonators are about 500.

V. Conclusion

A numerical method is presented for obtaining the resonant frequencies of open slot ring resonators. The analysis method is based upon Galerkin's method in the Hankel transform domain. The dependence of the solution on the choice of the basis functions is small. The numerical results obtained by this method agree with the experimental results within about 3 percent.

Acknowledgment

The authors would like to acknowledge the continuing guidance and encouragement of H. Sato, J. Kato, and K. Sawamoto. They also wish to express their gratitude to K. Onuki and Y. Shimoda for frequent, stimulating, and helpful discussions. Several useful suggestions for basis functions by M. Aikawa are gratefully acknowledged.

References

[1] S. Mao, S. Jones, and G. D. Vendelin, "Millimeter-wave integrated circuits," *IEEE Trans. Microwave Theory Tech.*, vol. MTT-16, pp. 455–461, July 1968.

[2] C. E. Fay and R. L. Comstock, "Operation of the ferrite junction circulator," *IEEE Trans. Microwave Theory Tech.*, vol. MTT-13, pp. 15–27, Jan. 1965.

[3] I. Wolff and N. Knoppik, "Microstrip ring resonator and dispersion measurement on microstrip lines," *Electron. Lett.*, vol. 7, pp. 779–781, Dec. 1971.

[4] Y. S. Wu and F. J. Rosenbaum, "Mode chart for microstrip ring resonators," *IEEE Trans. Microwave Theory Tech.*, vol. MTT-21, pp. 487–489, July 1973.

[5] T. Itoh and R. Mittra, "A new method for calculating the capacitance of a circular disk for microwave integrated circuits," *IEEE Trans. Microwave Theory Tech.*, vol. MTT-21, pp. 431–432, June 1973.

[6] T. Itoh and R. Mittra, "Analysis of a microstrip disk resonator," *Arch. Elec. Ubertragung.*, vol. 27, pp. 456–458, Nov. 1973.

[7] I. Wolff and N. Knoppik, "Rectangular and circular microstrip disk capacitors and resonators," *IEEE Trans. Microwave Theory Tech.*, vol. MTT-22, pp. 857–864, Oct. 1974.

[8] K. Araki and T. Itoh, "Hankel transform domain analysis of open circular microstrip radiating structures," *IEEE Trans. Antennas Propagat.*, vol. AP-29, pp. 84–89, Jan. 1981.

[9] K. Kawano and H. Tomimuro, "Slot ring resonator and dispersion measurement on slot lines," *Electron. Lett.*, vol. 17, pp. 916–917, Nov. 1981.

[10] J. A. Stratton, *Electromagnetic Theory*. New York: McGraw-Hill, 1941.

[11] J. B. Knorr and K. D. Kuchler, "Analysis of coupled slots and coplanar strips on dielectric substrate," *IEEE Trans. Microwave Theory Tech.*, vol. MTT-23, pp. 541–548, July 1975.

Kenji Kawano was born in Kitakyushu, Japan, on June 18, 1951. He received the B.S. and M.S. degrees in physics and applied physics from the Kyushu University, Fukuoka, Japan, in 1977 and 1979, respectively.

He joined the Musashino Electrical Communication Laboratory, Nippon Telegraph and Telephone (NTT) Public Corporation, Tokyo, Japan, in 1979, and has been engaged in the research of microwave integrated circuits. Recently, his major efforts have been directed toward millimeter-wave integrated circuits.

Mr. Kawano is a member of the Institute of Electronics and Communication Engineers of Japan.

Hisashi Tominuro was born in Kawasaki, Japan, 1949. He received the B.E. degree in control engineering from Tokyo Institute of Technology, Tokyo, Japan, in 1972.

He joined Musashino Electrical Communication Laboratories, Nippon Telegraph and Telephone Public Corporation, in 1972, and has been engaged in the research and development of the electronic components for transmission systems. He is presently engaged in the research and development of microwave integrated circuits for radio transmission systems. He is now a Staff Engineer of the Musashino Communication Laboratory, NTT Public Corporation, Musashino-shi, Japan.

Mr. Tomimuro is a member of the Institute of Electronics and Communication Engineers of Japan.